



HAL
open science

Substructure and strengthening of heavily deformed single and two-phase metallic materials

J. Gil Sevillano

► **To cite this version:**

J. Gil Sevillano. Substructure and strengthening of heavily deformed single and two-phase metallic materials. *Journal de Physique III*, 1991, 1 (6), pp.967-988. 10.1051/jp3:1991168 . jpa-00248644

HAL Id: jpa-00248644

<https://hal.science/jpa-00248644>

Submitted on 4 Feb 2008

HAL is a multi-disciplinary open access archive for the deposit and dissemination of scientific research documents, whether they are published or not. The documents may come from teaching and research institutions in France or abroad, or from public or private research centers.

L'archive ouverte pluridisciplinaire **HAL**, est destinée au dépôt et à la diffusion de documents scientifiques de niveau recherche, publiés ou non, émanant des établissements d'enseignement et de recherche français ou étrangers, des laboratoires publics ou privés.

Classification
Physics Abstracts
81.40L

Substructure and strengthening of heavily deformed single and two-phase metallic materials

J. Gil Sevillano

Escuela Superior de Ingenieros Industriales, Universidad de Navarra and C.E.I.T., Centro de Estudios e Investigaciones Técnicas de Guipúzcoa, San Sebastián, Spain

(Received 6 September 1990, accepted 15 October 1990)

Résumé. — Le durcissement par déformation des matériaux cristallins monophasés (et, dans une certaine mesure, des matériaux biphasés à grande dimension de phases, et des matériaux renforcés par une phase dispersée) à basse température résulte d'une compétition entre deux processus dynamiques : l'*accumulation de dislocations* pendant le glissement des dislocations sur de longues distances, et la *restauration dynamique*, comprenant des réarrangements locaux et des annihilations par réaction entre dislocations mobiles et accumulées. La compréhension complète de ces mécanismes serait très utile à la conception de matériaux de résistance optimisée par écrouissage. Cependant, la modélisation de l'évolution de la sous structure induite par déformation, qui est un ingrédient essentiel de toute théorie du durcissement, est encore loin d'être satisfaisante. Par ailleurs, certains composites *in situ* biphasés écrouis viennent juste après les whiskers parmi les matériaux métalliques les plus résistants. A première vue, le principal obstacle géométrique au glissement des dislocations dans les composites *in situ* lamellaires ou à fibres étant évident, on peut penser que leur résistance et leur durcissement sont parfaitement compris. Cependant, il n'en est rien et plusieurs écoles de pensée proposent diverses interprétations pour les écarts exagérés des courbes contrainte-déformation des composites *in situ*, par rapport aux courbes obtenues par la loi des mélanges. Le but de cet article est de discuter ces interprétations. Le composite Cu-Nb est choisi comme modèle, à cause de l'abondance des données mécaniques et microstructurales disponibles dans la littérature, pour diverses températures et chemins de déformation. La perlite fine Fe-Fe₃C est l'autre référence évidente.

Abstract. — Work hardening of single-phase crystalline materials (and to some extent, coarse two-phase and dispersion hardened materials too) at low temperatures results from the competition of two dynamic processes : *dislocation accumulation*, during the long-range gliding of mobile dislocations and *dynamic recovery*, involving local rearrangements and length annihilation from mobile and stored dislocation interactions. Its complete understanding would be very useful for designing materials with maximized strength after heavy cold work. However, modelling of the strain-induced evolution of the dislocation substructure, an essential ingredient of any work hardening theory, is still far from satisfactory. On the other hand, some heavily deformed ductile two-phase *in situ* composites are only second to whiskers among the strongest metallic materials. At first sight, the main obstacle geometry for dislocation glide in lamellar or multifilamentary *in situ* composites being clear-cut, it can be thought that their strength and work hardening are completely understood. However, this is not so and several schools of thought propose different interpretations for the exaggerated departure of the stress-strain curves of *in situ* composites from the rule-of-mixtures curves built from those of their bulk components. This paper aims to discuss such interpretations. The composite Cu-Nb is taken as model material owing to the extensive and

detailed mechanical and microstructural data available in the literature, including different deformation temperatures and two different strain paths. Fine pearlite Fe-Fe₃C is the other obvious reference.

1. Introduction.

Work hardening of single-phase crystalline materials at low temperatures results from the competition of two dynamic processes: *dislocation accumulation*, during the long-range gliding of mobile dislocations and *dynamic recovery*, involving local rearrangements and length annihilation from mobile and stored dislocation interactions. Dislocation accumulation is generally admitted to be an athermal process, dictated by the geometry and strength of the obstacle distribution to mobile dislocation glide. As the number of capture sites per unit surface scales with the mean dislocation density ρ and the length stored per site scales with the mean interdislocation distance, $1/\sqrt{\rho}$,

$$d\rho^+/d\varepsilon \propto \sqrt{\rho}. \quad (1)$$

On account of the fundamental relationship between the CRSS and the mean dislocation density,

$$\tau = \alpha Gb \sqrt{\rho} \quad (2)$$

equation (1) is equivalent to state that the work hardening rate (*), $\theta = d\tau/d\varepsilon$, is a constant, θ_0 , in the total absence of recovery processes and as far as the obstacle structure remains self-similar.

On the other hand, the dynamic recovery events leading to dislocation annihilation, $d\rho^-/d\varepsilon$, result from thermally activated processes.

At low and moderate strains (stage III) the microstructure consists of three-dimensional dislocation networks possessing a high capacity for dislocation capture. Simultaneous dynamic recovery so strongly counteracts dislocation storage that stage III would end in a saturation stress around $\bar{\varepsilon} \approx 1$. The behaviour is well described by a Voce-type work hardening equation [1]. In differential form,

$$\theta = \theta_0^{\text{III}}(1 - \tau/\tau_s^{\text{III}}) \quad (3)$$

where τ_s^{III} is a temperature and strain rate dependent saturation stress. However, after a threshold strain of such a magnitude, a transition takes place towards substructures that, despite their weak ability for dislocation capture, retain a positive strain hardening rate up to much higher strains, delaying the true saturation stress to values much higher than those extrapolated from stage III (Fig. 1). The transition marks the entry in the recently discovered « stage IV » of work hardening [5-9]. The actual macroscopic saturation stress once this stage is completed amounts to about $G/50$ at 0 K, instead of $G/80$ for the athermal value of the virtual saturation stress after completion of stage III [6]. BCC and some HCP metals (e.g., Ti) deformed by axisymmetric elongation (i.e., by wire-drawing) display an approximately linear stage IV that extends to much higher strains. This particular work hardening behaviour is linked to the continuous bending of their $\langle 110 \rangle$ or $\langle 1\bar{1}00 \rangle$ crystallites around the elongation

(*) The macroscopic work hardening rate is $\bar{\theta} = d\bar{\sigma}/d\bar{\varepsilon} = \bar{M}^2 \theta$, where \bar{M} is the appropriate orientation factor and $\bar{\sigma}$ and $\bar{\varepsilon}$ are the macroscopic stress and strain.

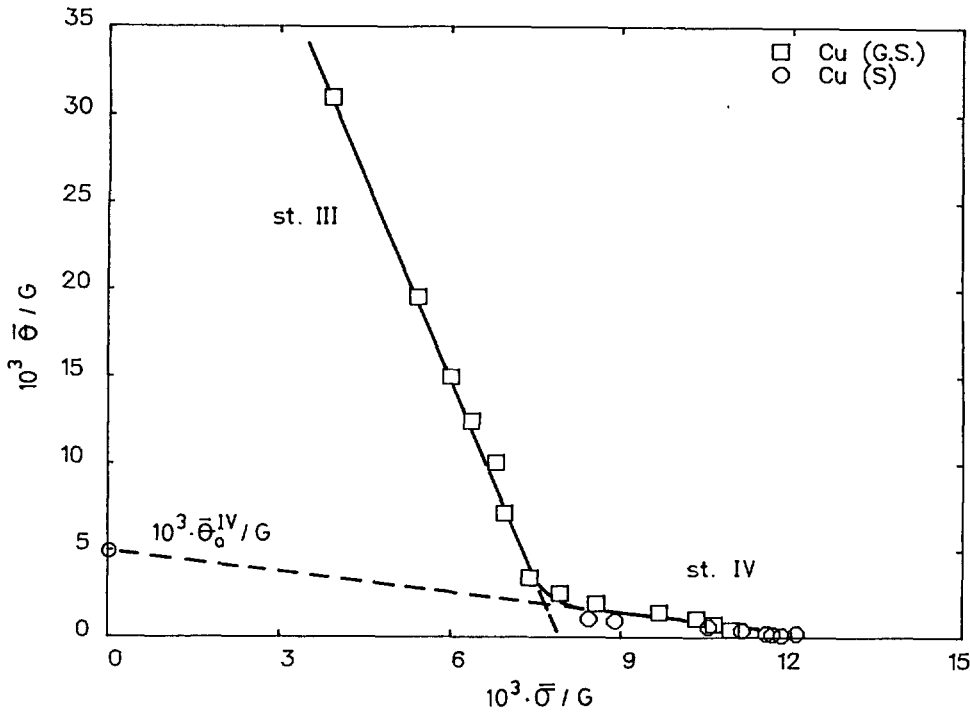


Fig. 1. — Work hardening rate of copper f (axisymmetric elongation) vs. tensile flow stress at room temperature, both normalized relative to shear modulus. Data from Gil Sevillano [2] (GS) and from Spitzig [3, 4] (S).

axis, tending to elongate by plane-strain. Such tilting needs the continuous storage of an excess of equal sign edge dislocations, difficult to remove by dynamic recovery at moderate temperatures. The saturation stress is then expected to be delayed to about $G/20$ or $G/15$ for the athermal limit [10]. Values of $G/33$ (Fe, Nb and W) and $G/25$ (Fe-6 %Si) have been quoted for the room temperature strength of BCC wires (see Ref. 10 for a tabulation). Figure 2 shows the work hardening rate vs. flow stress of niobium during axisymmetric elongation by room temperature wire drawing, superposed with the copper data of figure 1.

Raising the strength to very high levels has obviously much practical and theoretical interest and consequently the existence of the new work hardening stage, « stage IV », has received much attention during the last decade. Of course, understanding the transition from stage III to stage IV and the detailed mechanisms underlying the two competing processes of dislocation accumulation and dynamic recovery at work in stage IV would be very useful for mastering the design of materials with maximized strength after heavy cold work. As it is rather customary, practical knowledge has anticipated theory and from long ago it is known that heavily deformed ductile two-phase *in situ* composites are only second to whiskers among the strongest metallic materials. The strength records (4,9 GPa or $G/13$ at RT) — both absolute and relative —, still belong to the oldest and most common of them, pearlite [10], although recent interest has shifted to other two-phase systems — i.e. Cu/Nb — as a by-product of the development of Nb-based superconducting wires [13-15]. A very remarkable strength value of $G/19$ is probably the highest ever quoted for such system [14].

Studies on the work hardening, structure and physical properties of heavily deformed, ductile two-phase *in situ* composites were intensively conducted from 1970 by Wassermann,

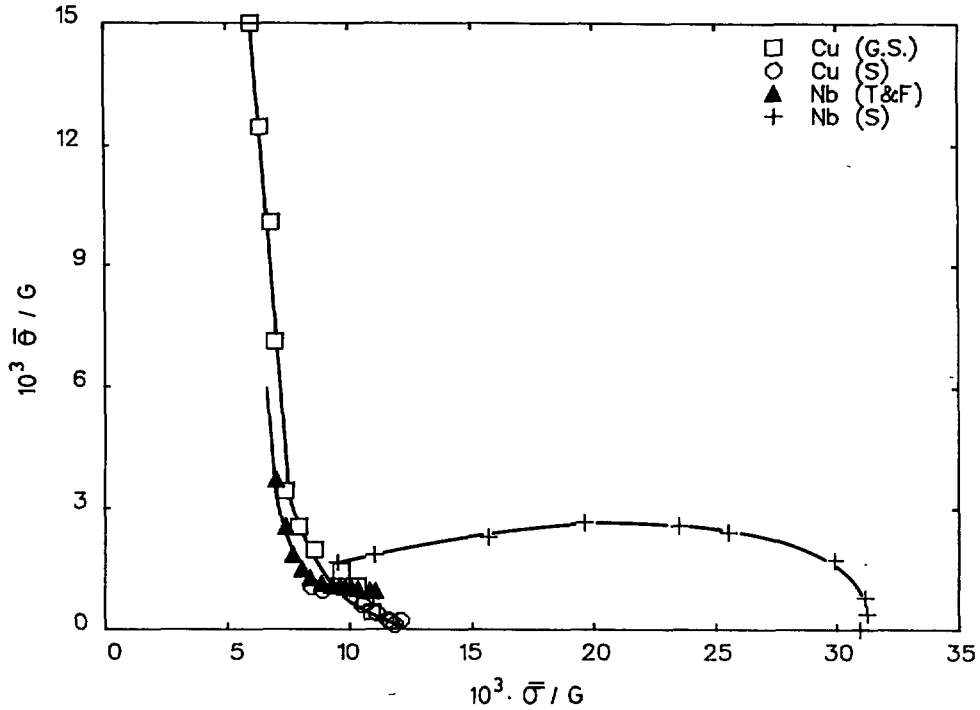


Fig. 2. — Id. figure 1, plus work hardening data of BCC niobium during wire drawing at room temperature. From data of Thompson and Flewitt [11] and Spitzig [3, 4]. Shear modulus and homologous temperature are 42.1 GPa and $0.216 T_m$ for Cu and 44.3 GPa and $0.107 T_m$ for Nb [12].

Frommeyer and co-workers [16-17] (for other references prior to 1978, see Ref. [5] of this paper), although a very interesting paper on an extremely deformed Cu-Nb composite ($\bar{\epsilon} \approx 25$) dates back to 1966 [18]. Mainly *via* eutectic compositions or other casting techniques or *via* powder metallurgy routes, FCC/FCC, FCC/BCC or even some metallic/non metallic mixtures (Ag-AgCl, Fe-MnS) have been prepared and successfully transformed in multifilamentary *in situ* composites. In all cases, an extraordinary enhancement of the work hardening rate (relative to that derived from the « rule-of-mixtures ») was observed, particularly for FCC/BCC systems transformed by wire-drawing, developing ribbon like BCC filaments with curled section or for rolled composites, developing fine lamellar structures too. In the latter cases, the work hardening curves are well described by an exponential of a fraction of the effective strain, $\bar{\epsilon}$, close to 1/4 (e.g., 1/5 for wire drawn Cu-20 %Nb or 1/3 to 1/4 for wire-drawn or rolled pearlite, Fig. 3) [20-24].

$$\theta \propto \bar{\sigma}/4 \rightarrow (\bar{\sigma} - \bar{\sigma}_0) \propto \exp(\bar{\epsilon}/4). \quad (4)$$

Why are *in situ* composites so strong? A qualitative answer is easy. The flow stress of work hardened single-phase materials is determined by dislocation-dislocation interactions and, as referred above, an inherent dynamic softening process is active simultaneously with the hardening associated to plastic flow. Introducing in the substructure extrinsic long-range obstacles for dislocation glide, immune to dynamic recovery, means in some way to become independent from the shortcomings of the work hardening process of the bulk matrix. If the extrinsic obstacles consist of a ductile second phase, plastic deformation increases the obstacle

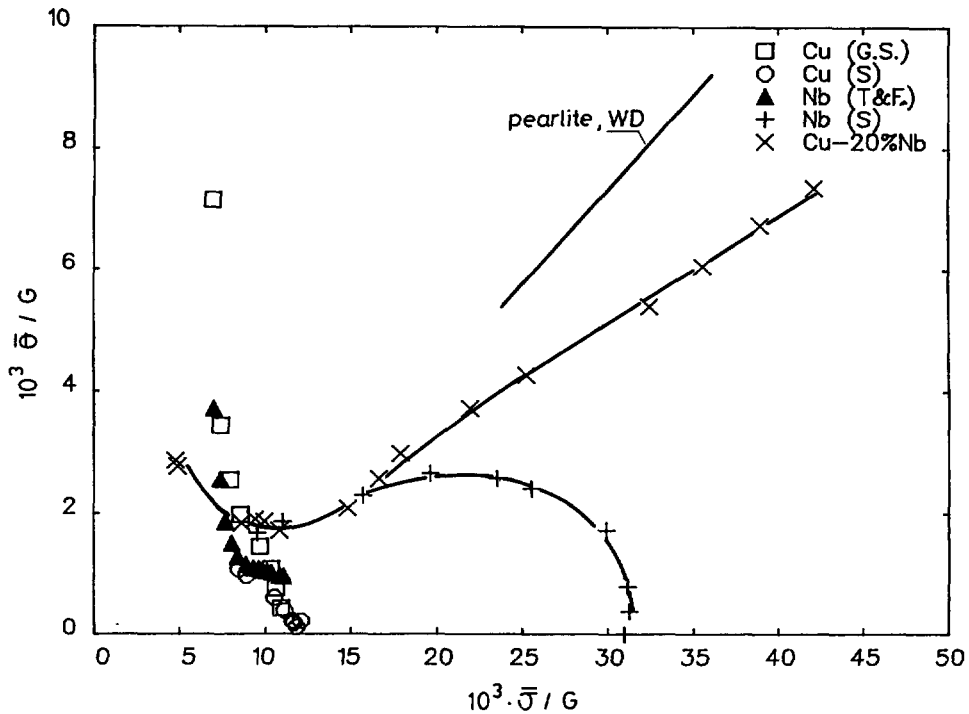


Fig. 3. — Work hardening rate vs. flow stress of two *in situ* composites during straining by axisymmetric elongation. Derived from data of Spitzig *et al.* [3, 4] and Riveros [19].

density. When the latter is high as in the *in situ* composites, it can control the flow stress and the work hardening of the material, whose strength can be raised up to the limits imposed by technology, exhaustion of ductility or instability of the composite microstructure. However, there is no consensus on the detailed mechanisms responsible for their work hardening process.

The less developed ingredient of a complete work hardening theory for single-phase metals is the modelling of substructural evolution. At first sight, the obstacle geometry of lamellar or multifilamentary *in situ* composites being clear-cut, it can be thought that their strength and work hardening are completely understood. However, this is not so and several schools of thought propose different interpretations for the exaggerated departure of the stress-strain curves of *in situ* composites from the rule-of-mixtures curves built from those of their bulk components. As it has been pointed out [24] the discussion is almost a repetition of the older one on pile-up and non pile-up theories for the Hall-Petch grain size flow stress relationship, with a group of authors emphasizing the direct rôle of the second-phase barriers in the composite strengthening and another one favouring models based on the enhanced dislocation storage of the deforming composite due to the presence of the second-phase. This paper aims to discuss such interpretations. The composite Cu-Nb and fine pearlite are taken as model materials owing to the extensive and detailed mechanical and microstructural data available in the literature including different deformation temperatures and different strain paths.

2. Models for the strength of heavily cold worked *in situ* composites.

2.1 THE RULE OF MIXTURES. — It is frequently emphasized the amazing departure of the stress-strain behaviour of *in situ* composites from the « rule of mixtures » (ROM),

$$\bar{\sigma} \gg f_1 \bar{\sigma}_1 + (1 - f_1) \bar{\sigma}_2 \quad (5)$$

where $\bar{\sigma}_1$ and $\bar{\sigma}_2$ represent the strengths of the two phases of the composite for the same strain level. *In situ* composites already start with a quasi-continuous lamellar structure (lamellar eutectics and eutectoids, multi-layer structures) or they develop it during large straining. Such continuity or, at least, the very high aspect ratio of the discontinuous phase with lesser volume fraction, assure the validity of the isostrain approximation for the behaviour of the composite. Isostrain ROM in accordance with plasticity theorems, should provide an upper-bound for the composite strength, in apparent contradiction with the inequality (5). The contradiction disappears if it is realized that the individual strengths of the two phases to be entered in the ROM are not those corresponding to the stress-strain curves of the bulk phases but the strengths of very thin layers of material bounded by extended interfaces and probably suffering from effects of strain compatibility with neighbouring alien material. Therefore, all models for the stress-strain behaviour of *in situ* composites rely on the use of the ROM with modified individual phase strengths and they can be classified in two groups according to the main reason invoked for explaining the departure of the local behaviour of the layers or filaments embedded in the composite from their bulk material behaviour :

- a) *enhanced dislocation storage*, arising from
 - reduced mean free path
 - geometrically necessary dislocations
- b) *direct effect of the presence of interphase barriers*, such as
 - Hall-Petch type (pile-up) effects
 - interlamellar bowing of dislocations for gliding or for dislocation multiplication
 - internal stresses associated to the presence of interfaces or interfacial dislocations.

2.2 INTERPHASE SPACING vs. MEAN FREE PATH OF DISLOCATIONS. EXPECTED EFFECTS ON THE COMPOSITE BEHAVIOUR.

2.2.1 *The undisturbed mean free path of dislocations.* — For a single-phase crystal, a virtual dislocation « mean free path », L , can be defined as the distance to be covered by a dislocation of unit length in order to store a unit length of dislocation [1, 26-28]. It can be anticipated that when the spacing, S , of the components of the *in situ* composite is much higher than its dislocation « mean free path », $S \gg L$, their work hardening rate will be undisturbed relative to its bulk single-phase behaviour and then — in the absence of other possible superposed effects to be discussed in the following — the simple ROM will hold. When $S \approx L$, dislocation storage at the interfaces or in the lamellae will be comparable, and probably an enhancement of dislocation storage will be observed. Finally, when $S \ll L$, a strong « size effect » in the behaviour of the phase is predicted, with dislocation storage at the interior of the lamellae reduced or even suppressed (when $S < 1/\sqrt{\rho}$).

To be consistent with the work hardening picture presented above (see Introduction), the virtual mean free path should be linked to the athermal rate of dislocation accumulation, θ_0 . According with the definition of L and making use of equation (2), it results

$$L = \alpha^2 b/2(\theta_0/G)(\tau/G). \quad (6)$$

Table I. — *Athermal extrapolations of experimentally measured work hardening rates.*

	$10^3 \theta_0^{\text{III}}/G$	$10^3 \theta_0^{\text{IV}}/G$	Def. mode	Ref.
1 050 Al	6.4	0.28	torsion	Alberdi (1984) [6]
ETP Cu	4.5	0.39	torsion	Alberdi (1984) [6]
SS 321	3.2	0.40	torsion	Alberdi (1984) [6]
Fe-0.07 % C	8.7	—	torsion	Gil Sevillano <i>et al.</i> (1980) [5]
Fe-0.007 % C	—	0.47	wire drawing	Langford (1966) [29]

Elastic constants from Kocks (1976) [1] and Frost and Ashby (1982) [12].

Orientation Factors : $M_{\text{III}} = 1.67$ and $M_{\text{IV}} = 1.50$ for FCC (torsion) and $M_{\text{III}} = 1.50$ and $M_{\text{IV}} = 3.0$ for, respectively, BCC torsion and wire drawing.

Values of θ_0 for three FCC metals and for low carbon steel are given in table I. For large strain behaviour, θ_0^{IV} values are to be retained. The high value of θ_0^{IV} for ferrite deformed by wire drawing — estimated from work hardening curves at two drawing temperatures (from Ref. [29]) shows the effect of the extra accumulation of dislocations arising from the curling of the $\langle 110 \rangle$ grains and it is expected to be representative of other BCC metals.

To compare with the spacings of heavily deformed multifilamentary Cu-Nb composites, L values of Cu, Nb and Fe computed according to equation (6) and data of table I are presented in table II.

2.2.2 *Microstructural evolution of in situ composites at large strains.* — The mean transverse spacing of the two phases of heavily strained *in situ* composites produced by wire drawing or rolling evolves approximately according to

$$\bar{s}_T/\bar{s}_0 \approx \exp(-0.5 \varepsilon) \quad (7)$$

Table II. — *Virtual « mean free path » of dislocations in copper, niobium and iron at large strains (Eq. (6), stage IV, axisymmetric elongation by wire drawing). Room temperature.*

	$10^4 \theta_0^{\text{IV}}/G$	$10^3 \tau^{\text{IV}}/G$	b (μm)	α	L (μm)	$1/\sqrt{\rho}$ (μm)
Cu	4	2.5 → 3.6 (*)	2.56×10^{-4}	0.35	16 → 11	0.036 → 0.025
Nb	5	3 → 10 (*)	2.86×10^{-4}	0.35	12 → 3.5	0.034 → 0.01
αFe	5	7.8 → 28 (**)	2.48×10^{-4}	0.35	3.9 → 1.1	0.011 → 0.003

(*) τ_s^{IV} .

(**) $\tau(\varepsilon = 10) < \tau_s^{\text{IV}}$.

where \bar{s}_0 is the mean spacing of the starting phases and ε the longitudinal strain. Under the plane strain elongation macroscopically imposed in rolling or locally developed in drawing of BCC materials, a $\bar{s}_T/\bar{s}_0 \approx \exp(-\varepsilon)$ dependence should be expected. However, equation (7) has been observed to hold for many different two-phase systems: Fe-Fe₃C pearlite [20-22] Cu-Nb [3, 4, 31, 32], Cu-Ta [33], Ag-Ni, Cu-Fe, Cu-Cr, Ni-W [34]. The deviation of the local strain of the composite from plane strain in transverse sections is better understandable in wire drawing (from the interaction among neighbouring grains or colonies [22]) than in rolling, where no local accommodation of the « curling » type is necessary. The profuse activity of intense shear bands could offer an explanation. Signs of such activity — in the form of intensive fragmentation of the lamellae — are sometimes evident in longitudinal sections of rolled *in situ* composites [22, 35].

Detailed measurements made on oriented pearlite [22] can be very well fitted to equation (7), both for rolling or for wire drawing. For Cu-20 %Nb, the results are [4, 31]:

$$\bar{s}_T/\bar{s}_0 \approx \exp(-0.36 \varepsilon) \quad (8)$$

for the wire drawn composite and

$$\bar{s}_T/\bar{s}_0 \approx \exp(-0.74 \varepsilon) \quad (9)$$

for the composite produced by rolling. There is little more than the qualitative explanations referred above to justify the geometrical evolution of the cross sections of the microstructures of *in situ* composites and in this respect, modelling of their work hardening behaviour suffers from the same limitation encountered in the development of single-phase work hardening theories.

The starting values of the spacings, S_0 , can broadly differ. Fine Fe-Fe₃C pearlite produced by solid-state eutectoid decomposition at the lowest temperature that yields a lamellar structure (~ 550 °C) starts with $S_0(\text{Fe}) \approx 0.07$ μm , $S_0(\text{Fe}_3\text{C}) \approx 0.01$ μm . Niobium, tantalum, chromium, etc., dendrites produced *via* more or less conventional casting or powder metallurgy routes in a copper matrix have a thickness $S_0(\text{Nb}) \approx 3 \div 8$ μm , i.e., for a 20 % vol Nb, $S_0(\text{Cu}) \approx 12 \div 32$ μm . The high ductility of copper-based composites allows to deform them up to $\varepsilon = 12$ by wire drawing. The limit for wire drawing of fine pearlite is set at $\varepsilon = 5$. The difference of two orders of magnitude in their initial microstructure scales cannot be compensated by their present different limit strains.

2.2.3 Comparison of the spacings of *in situ* composites with the mean free path of dislocations.

— The spacings of the wire-drawn or rolled Cu-20 %Nb composites of Spitzig *et al.* [4, 31] can be now compared with the Cu and Nb mean free paths and mean interdislocation distances (Tab. II). At large strains ($\varepsilon > 4$) and up to the maximum strains reported, for $\bar{S}_0(\text{Cu}) = 24.8$ μm and $\bar{S}_0(\text{Nb}) = 6.2$ μm ,

$$\begin{aligned} 5.9 > \bar{S}_T(\text{Cu})_{\text{WD}} > 0.3 \mu\text{m} & \quad 1.5 > \bar{S}_T(\text{Nb})_{\text{WD}} > 0.08 \mu\text{m} \\ 1.3 > \bar{S}_T(\text{Cu})_{\text{R}} > 0.15 \mu\text{m} & \quad 0.3 > \bar{S}_T(\text{Nb})_{\text{R}} > 0.04 \mu\text{m} . \end{aligned}$$

Comparing with the L and $1/\sqrt{\rho}$ values of table II,

— the gliding distance of dislocations is reduced relative to their « mean free path » for both materials, particularly during rolling. The interfaces will receive (not necessarily store !) a dislocation density per unit strain higher than the density accumulated in the interlamellar volume ;

— the intralamellar dislocation storage (and work hardening process) of Cu is probably

unaffected (no size effect) as the spacing remains — if the last rolling stage is excepted — above ten times the interdislocation spacing.

— Niobium spacings are — at least for high strains — below ten times the interdislocation distance $1/\sqrt{\rho}$ that would develop for large-size crystals. Consequently, the « normal » dislocation pattern cannot be built and the work hardening rate is probably perturbed (decreased).

In fine pearlite, the thickness of the ferrite lamellae are approx. 50 times lower than the mean free path of dislocations and below ten times the mean interdislocation distance that would develop under free gliding conditions. The statistical storage of dislocations in the interlamellar volume will be irrelevant relative to the dislocation capture on the interfaces. The thickness of the lamellar cementite crystals is so extreme (from 10 nm to 0.8 nm in the $0 \leq \epsilon \leq 5$ range) that any consideration of their virtual work hardening seems meaningless. A lattice-friction controlled strength or a whisker-type behaviour seems more plausible for them.

Ten times the mean interdislocation distance equals approximately the size of the cellular or subgranular dislocation structure induced by single-phase plastic deformation [5]. Theoretical models developed up to now for large strain work hardening of single-phase materials (stage IV) have in common the assumption of ascribing dislocation accumulation to the cellular walls, the capability of dislocation storage in cell interiors being exhausted at the end of stage III. Then it is meaningful to compare the microstructural size of heavily deformed *in situ* composites with the cellular size induced in their components under free slip

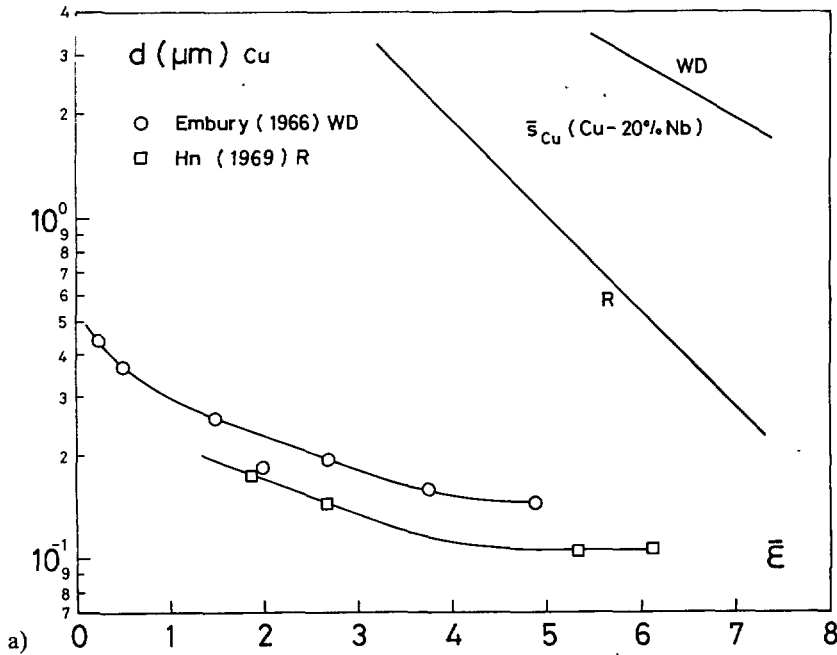


Fig. 4. — Cellular size, d , induced by free slip plasticity in Cu, Nb and Fe compared with their spacings in heavily strained *in situ* composites deformed by wire-drawing (WD) or rolling (R). a) Cu-20 % vol. Nb [4, 31]. Copper data from Embury *et al.* [36] and Hu [37]. b) Cu-20 % vol. Nb. [4, 31]. Niobium data from Thompson and Flewitt [11]. c) Fe-Fe₃C fine pearlite [22]. Ferrite data from Langford and Cohen [38] and Rack and Cohen [39].

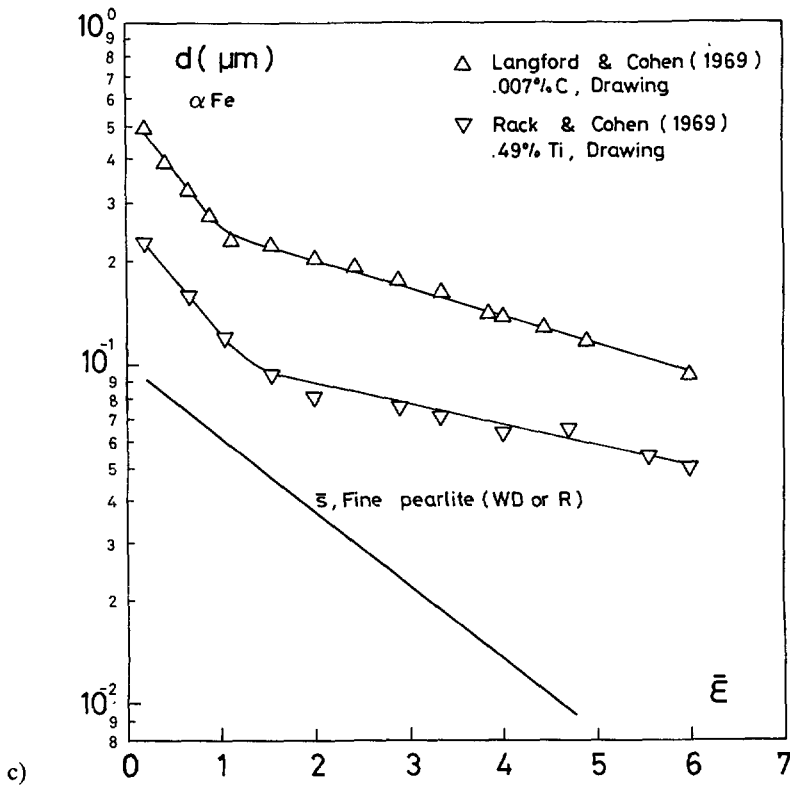
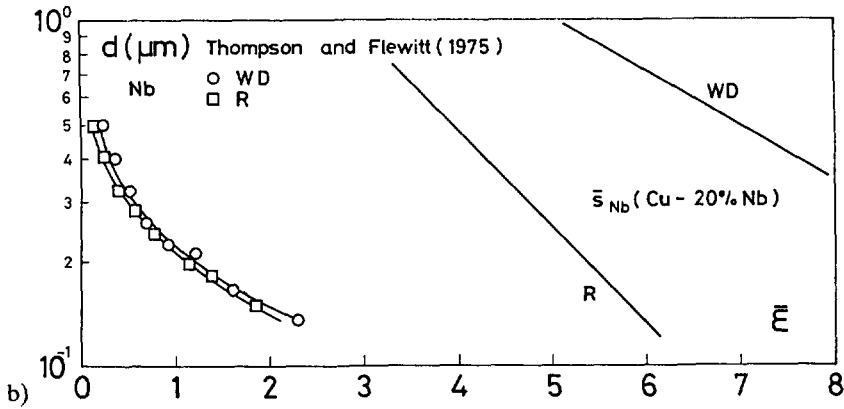


Fig. 4 (continued).

conditions. This is done in figures 4a-c for Cu-Nb and for fine pearlite. This alternative comparison of microstructural sizes corroborates some of the previous conclusions :

— A cellular substructure of dislocations can develop in the copper matrix and in the niobium ribbons of Cu-Nb composites. Only at the highest strain level attained by rolling the thickness of niobium (and copper in a lesser extent) will enter in conflict with the free cellular size.

— There is no chance for developing the cellular dislocation substructures of polycrystalline ferrite inside the ferrite lamella of fine pearlite. On the basis of the currently accepted ideas about dislocation patterning, only walls transverse to the interfaces seem probable.

2.2.4 Experimental evidence on dislocation substructures and densities. — Several experimental observations appear to confirm the predictions derived from the comparison of the composite spacings with the substructural scale of similarly strained pure metals. Qualitatively, the wire drawn or rolled composites display in the Cu matrix or in the Nb ribbons the same low-energy dislocation structures found in stage-IV of pure metals [4, 31]. No statistically representative measurements are available to ascertain about quantitative differences. On the other hand no resolvable cellular dislocation structure can be seen in transverse ferrite sections of heavily deformed fine pearlite [22].

There is some disagreement on measured dislocation densities. Resistivity and TEM measurements [40, 25] yield very high values for Cu-Nb composites, up to 10^{13} cm^{-2} . Some other direct TEM measures have given much lower values, 10^{10} cm^{-2} , but they correspond only to cell interiors [4], i.e., the high local density in the cellular walls has been excluded. Inclusion of the latter and account of the contribution of interfaces to electrical resistivity [41] could reconcile the two values. Only for very high strains the Nb filaments become denuded of dislocations [4, 31], once their thickness has attained very low values. A similar effect had been earlier noticed in wire drawn Ag-Cu composites [17] and, as mentioned, it is evident in fine pearlite from the beginning of its deformation.

2.2.5 Conclusion on the contribution of matrix or intralamellar « normal » work hardening to the composite strength. — The conclusion of this section is that intralamellar work hardening of the component materials of Cu-Nb and other similar composites — whose starting structure is relatively coarse — forms the base-line on which other possible mechanisms will superpose to build the total strength of the composite. The simple ROM represents then a lower bound for strength prediction. Only after very large strains the intralamellar work hardening will tend to disappear in the Nb ribbons.

For fine pearlite, the intralamellar work hardening contribution will be negligible.

2.2.6 Strain hardening by dislocation storage at the interfaces. — After crossing each phase of the composite, dislocations come to the interface, where they will be partially absorbed. Some fraction, K , of them might be stored at the interface, either because the latter cannot act as perfect dislocation sink or because some heterogeneity of strain is to be accommodated. The rate of interfacial dislocation storage will then be :

$$d\rho/d\Gamma = 2 K/b\bar{S}, \quad K < 1. \quad (10)$$

Where \bar{S} is the mean spacing on the considered slip plane (*). Accounting for equation (7) and using the appropriate orientation factor, M , integration of equation (10) leads to :

$$\rho \simeq \rho^* + (MK/b\bar{S}_0) \exp(\varepsilon/2) \quad (11)$$

where ρ^* should include the initial plus the statistically stored dislocation density between the

(*) On a particular slip plane and assuming a perfect lamellar morphology, $S = S_{\min}/\sin \lambda$, S_{\min} being the minimum local spacing, i.e., the spacing measured in a direction normal to the lamellae and λ the angle between the lamellae and the slip plane. At large strains, when the structure is strongly oriented, $\bar{S}_{\min} = 2 \bar{S}_T/\pi$ for the wire drawn composite and $\bar{S}_{\min} = \bar{S}_T$ for the rolled one (measured in the short-transverse direction, i.e., normal to the rolling plane).

interfaces. At large strains, it may be assumed that the second term will dominate and then [24]

$$\begin{aligned}\sigma &\approx \bar{\alpha} G \sqrt{MKb} / \sqrt{\bar{S}_T} \\ &\approx \alpha G \sqrt{MKb/\bar{S}_0} \exp(\varepsilon/4).\end{aligned}\quad (12)$$

The predicted work hardening rate formally agrees with the observed behaviour, equation (4). Moreover, a Hall-Petch type relationship between the flow stress and the spacing is predicted, too. But, although such a relationship is most frequently used to fit $\bar{\sigma} - \bar{S}_T$ experimental data, in the case of Cu-20 %Nb composites it is clear that the true $\bar{\sigma} - \bar{S}_T$ relationship of the rolled composite is not at all of the Hall-Petch type [31, 42]. This conflict with the observed facts and the unlikely high value of the K factor needed to fit the behaviour of the wire-drawn composite cast serious doubts about the validity of this explanation for the work hardening of *in situ* composites.

2.3 EFFECTS OF COMPATIBILITY STRAINS : GEOMETRICALLY NECESSARY DISLOCATIONS. — Courtney and coworkers [43, 44] have developed an elaborated model for the strain hardening of *in situ* composites based on the accumulation of « geometrically necessary dislocations » [27] assuring the compatible straining of the two phases. In each phase, dislocations must be stored in order to allow some deviation from the perfect isostrain ; in the simplest case, such deviation can be assumed to be a small fraction, C , of the global strain increment of the composite :

$$d\rho_G = C d\Gamma/b\bar{S} = CM d\varepsilon/b\bar{S}, \quad C \ll 1. \quad (13)$$

On account of the strain refinement of the microstructure, equation (7), and in the total absence of dynamic recovery,

$$\rho = \rho_s + (CM/2 b\bar{S}_0) \exp(\varepsilon/2)$$

where ρ_s represents the statistical dislocation storage. This equation, formally identical to equation (11), leads to similar results for large strains (Eq. (12)). The absence of dynamic recovery is obviously an oversimplification and, in fact, the model takes into account the activity of dynamic recovery processes. For the free phase, a Voce type behaviour is assumed :

$$(d\rho/d\varepsilon)_{s.ph.} = C_1 \sqrt{\rho} - C_2 \rho. \quad (14)$$

The first term represents the athermal-statistical-accumulation, equation (1), and the second one the thermally activated dynamic recovery. Equation (14) is equivalent to equation (3) on account of equation (2). For a given temperature and strain rate, the constants C_1 and C_2 are obtained from the large strain (i.e., stage IV) behaviour of the single phase. Then, the statistical accumulation of dislocations and the dynamic recovery activity of the phase are assumed to remain unmodified in the composite, where the compatibility term, equation (13), represents an extra input of dislocations :

$$d\rho/d\varepsilon = C_1 \sqrt{\rho} - C_2 \rho + CM/b\bar{S}. \quad (15)$$

The strength of the composite is computed from the modified ROM assuming equation (15)

particularized for each phase. The two C values are adjusted to give the best fitting with the experimental strain hardening of the composite (*).

The results of the model are very impressive in reproducing the shape of the strain hardening curve of several composites but the values of the « mismatch » parameters, C , of the two phases cannot, up to now, be predicted. Moreover, the model cannot avoid severe criticisms. To begin with, it presumes that the processes of accumulation of dislocations and dynamic recovery do not suffer of any size-effect in the composite which, as it has been previously discussed, is very unlikely after large strains. Furthermore, it makes no distinction between the statistically stored dislocations, enduring dynamic annihilation processes associated to their spatial pattern (three-dimensional structures) and the « mismatch » dislocations, most probably spread on the planar interfaces of the lamellar structure, neither subject to the same low temperature recovery processes nor generating similar strengthening effects. Finally, the model rather surprisingly presumes an enhancement of work hardening in both phases of the composite because of the extra accumulation of geometrically necessary dislocations (i.e., both C_1 and C_2 are assumed positive), instead of adopting the more natural hypothesis of the harder phase deforming less than the softer one.

2.4 HALL-PETCH (PILE-UP) THEORIES. — Combining the empirical equations (4) and (7), a Hall-Petch type relationship results between the composite strength and the transverse spacing of its microstructure. This has been recurrently justified in many occasions on the basis of pile-up models (e.g., Refs. [14, 20]). Assuming phase 2 is harder than phase 1 and that double-ended pile-ups built in 1 because of its confined flow (blocked by the interfaces), plastic flow at the interface will be induced when [45]

$$\tau_1 - \tau_0 \approx S_1^{-1/2} \sqrt{2 G_1 b_1 \tau_2 / \tau} . \quad (16)$$

Empirical Hall-Petch slopes for *in situ* formed composites [3, 4, 20, 31, 33, 42, 46] range from 0.3 to 3 MPa m^{-3/2}. It can be checked using equation (16) and the appropriate orientation factor that such high values are only compatible with equation (16) if the hard component behaves as a whisker, i.e., with $\tau_2 \approx G/15$. Such a behaviour is plausible for the extremely thin cementite lamellae in fine pearlite, but very questionable for the Nb ribbons in Cu-Nb composites, where a dislocation substructure is evident.

Some other experimental observations are difficult to reconcile with a pile-up model. Different Hall-Petch slopes are obtained for the same Cu-20 % vol Nb combination depending on the deformation mode (rolling or wire drawing) [42]. In fact, the rolled composite does not display any Hall-Petch behaviour at all [31]. Also, the well developed cellular, subgrain or even micrograin substructures observed in the copper lamellae of the Cu-Nb composites [4, 41] make unlikely a virtual control of their strength by intralamellar pile-ups.

2.5 CRITICAL STRESS FOR INTRALAMELLAR DISLOCATION GLIDING OR FOR DISLOCATION MULTIPLICATION.

2.5.1 The lowest bound: critical stress for intralamellar dislocation gliding. — With incoherent interfaces, dislocation glide on the slip plane bounded by two impenetrable, parallel interfaces needs the bowing of the dislocation up to the critical configuration

(*) To compare with the nomenclature of Courtney *et al.* [43, 44], it is to be noted that, for phase A : $P_A K = M_A C_A / b_A$. And for phase B : $(1 - P_A) K = M_B C_B / b_B$.

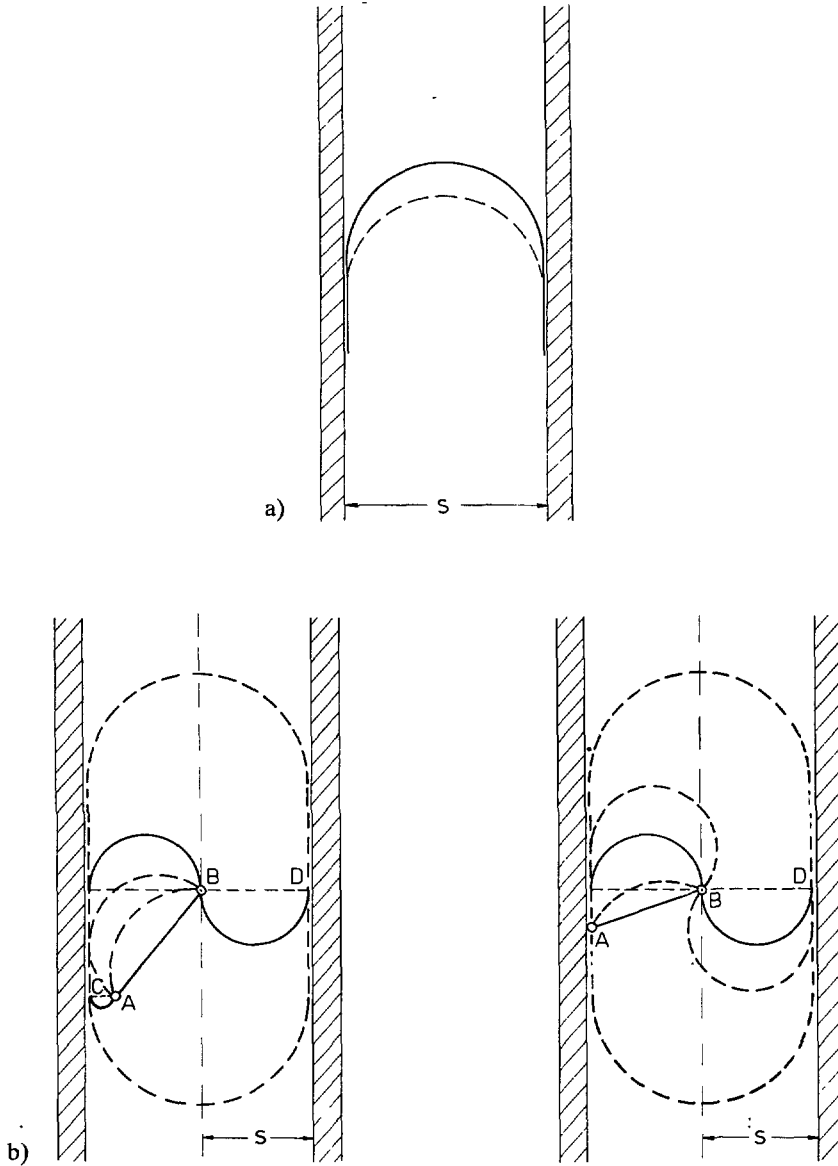


Fig. 5. — a) Gliding of a dislocation between two impenetrable interfaces, b) the softest dislocation mill for intralamellar multiplication of dislocations [47, 48].

(Fig. 5a). With the fixed-line tension simplification, the critical shape is semicircular and the stress to attain it is

$$\tau_b = (AGb/2 \pi S) \ln (S/b), \quad A \approx 1.2. \quad (17)$$

This represents the absolute lower bound for the CRSS of a lamellar component. When interfacial dislocation sources are available and the density of dislocations is very low, τ_b controls the composite strength. One example of such situation is the elastic limit of as transformed pearlite [47].

2.5.2 *The lower bound for activation of intralamellar dislocation sources.* — When interfacial dislocation sources are exhausted, multiplication of dislocations in the concerned phase of the composite shall take place by activation of dislocation mills in the intralamellar channels. The softest sources in such situation correspond to dislocation segments of length over half the interlamellar distance, $S/2$ and with one end anchored in the middle of the lamella (Fig. 5b) [47, 48]. The critical stress for such configuration is

$$\tau_m = (AGb/\pi S) \ln (S/2 b), \quad A \approx 1.2 \quad (18)$$

i.e., approximately twice τ_b , equation (17). This critical stress for dislocation multiplication appears to govern the ferrite strength in heavily deformed pearlite [47], see section 3.2 below.

2.6 INTERNAL STRESSES. — Geometrically necessary dislocations induced to absorb compatibility strains in an *in situ* composite with layered structure, i.e., with extended, planar interfaces are more likely producing internal stresses than acting as local obstacles to intralamellar dislocation glide. They cannot probably be distinguished from the dislocation density captured by the interfaces. They can be viewed in the Ashby sense [27] — absorbing the misfit — or as the local stress risers making possible the plastic straining of the harder phase under an effective macroscopical stress below the strength of that phase. On account of force equilibrium in the two phase composite and of the balance of external an internal plastic works, such internal stresses can be disregarded for computing the composite flow stress if the ROM is applied with the actual strengths of the individual phases in the composite, i.e., accounting for the constraints imposed by the presence of the lamellar interfaces.

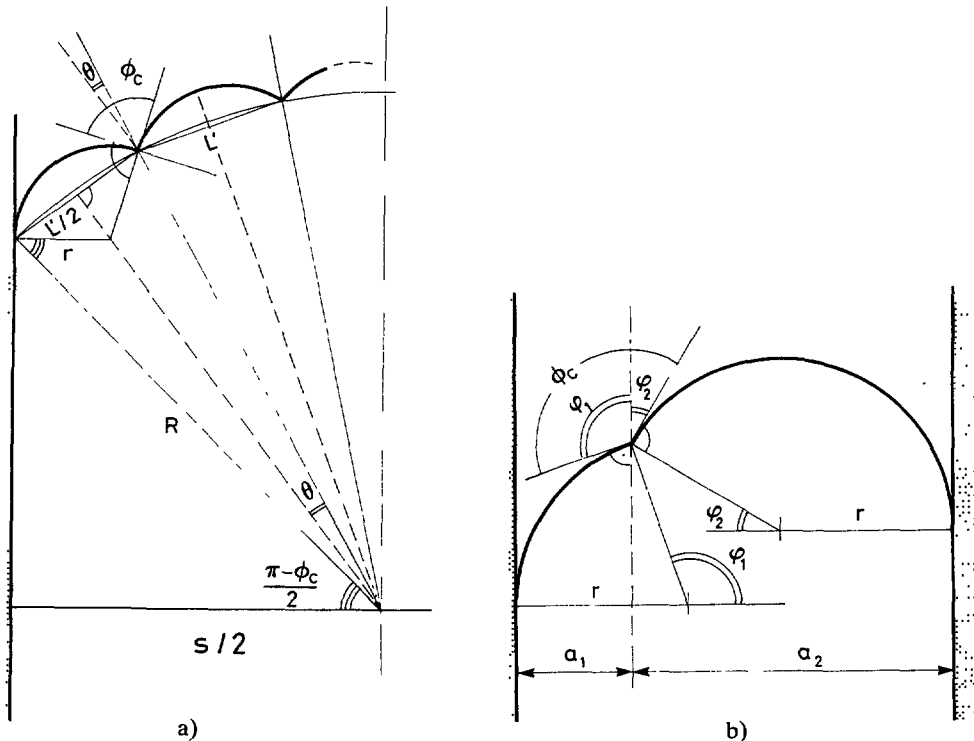


Fig. 6. — a) Critical configuration for driving a dislocation between two non-penetrable walls on a slip plane containing a regular distribution of point obstacles. b) Id., for very low point obstacle density.

The difference of elastic constants of the two phases of the composite produces image forces on the dislocations — more intense at the proximity of the interface — and their effects are akin to internal stresses [49, 50]. In the case of pearlite or Cu-Nb composites, the elastic heterogeneity, at least on the basis of the isotropic values of the elastic constants, is low. No attempt has been made up to now to include the image force contribution to the strength of those *in situ* composites.

2.7 SUPERPOSITION OF EFFECTS. — As a first approximation, friction or internal stresses will make an additive contribution that we will include in a generic base-line τ_0 . On the other hand, dislocation gliding through the intralamellar channels or activating intralamellar sources needs the critical bowing of the dislocation line for advancing tangent to the lamellar wall while simultaneously overcoming the obstacles on its slip plane, i.e., in our case, the dislocation density stored in the ribbon of the phase under consideration. An estimation of such critical stress can be gained from the simplified regular geometry of figure 6a :

$$\begin{aligned} \tau - \tau_0 &= (Gb/L') \cos [\varphi_c/2 - \arcsin [L'(\varphi_c/2)/S]] \\ &\approx \tau^* \sin^2 (\varphi_c/2) + \tau_{\text{obst.}}, \quad S/L' > 2. \end{aligned} \quad (19)$$

Where τ^* is τ_b or τ_m (in the absence of obstacles) and $\tau_{\text{obst.}}$ the critical stress for passing through the obstacle field without any restrictions to the mean free path. L' is the mean effective distance between obstacles, i.e., the Friedel's distance,

$$L' = L / \sqrt{\cos (\varphi_c/2)}, \quad L = 1 / \sqrt{\rho}. \quad (20)$$

For a distributed density of dislocations, $\varphi_c \approx 100^\circ$, and then

$$\tau - \tau_0 \approx 0.6 \tau^* + \alpha Gb \sqrt{\rho}. \quad (21)$$

For weaker obstacle densities, figure 6b,

$$\tau^* \leq \tau - \tau_0 \leq [1 + \cos (\varphi_c/2)] \tau^*, \quad S/L' \approx 2. \quad (22)$$

3. Application : work hardening of pearlite and Cu-20 %Nb composites.

3.1 ORIENTATION FACTORS. — Equations (16)-(18) predict values of the CRSS linearly dependent on S^{-1} or $S^{-1/2}$, with S the spacing measured on the slip plane, i.e., $S = S_{\text{min}}/\sin \lambda$ (see footnote on section 2.2.6). Consequently, the CRSS values are not uniform for the different slip systems. Then, an orientation factor, M^* , can be defined as :

$$\tau_i = k/S_i^m, \quad \sigma d\varepsilon = \sum \tau_i d\Gamma_i, \quad \bar{\sigma} = M^*(k/S_{\text{min}}^m) \quad (23)$$

with $m = 1$ or $m = 1/2$, depending on the equation relating the CRSS with the spacing [51]. When the CRSS has a non-negligible component independent from the spacing S of the different systems (Eq. (19)), a good approximation [51] for deriving the macroscopic flow stress is :

$$\bar{\sigma} \approx \bar{M}[\tau_0 + \tau(\rho)] + 0.6 M^*(k/S_{\text{min}}^m). \quad (24)$$

Where \bar{M} is the orientation factor for uniform CRSS values. Without using the correct orientation factors, any quantitative checking of work hardening models for *in situ* composites against experimental results cannot be attempted.

Ribbons formed by BBC crystals when wire drawing bulk BCC metals or BCC-containing *in situ* composites have a {001} <110> orientation (respectively, lamellar plane and wire axis). Assuming a $\tau^* \propto S^{-1}$ relationship and {110} {112} <111> slip, the range of $\sin \lambda$ values (i.e., the relative range of CRSS values) goes from 0.577 to 1. A Taylor-type calculation (full constraints) [52] gives for the tensile deformation of such ribbons $M^* = 1.84$.

Most Nb lamellae in rolled Cu-Nb composites develop a {113} <110> preferred orientation [31, 42] (same convention as before) coincident with the main component of the Nb rolling texture [53]. Assuming a $\tau^* \propto S^{-1}$ relationship, the relative range of CRSS values goes from 0.52 to 1. The Taylor-model calculation (full constraints) gives for the orientation factor in axisymmetric tension $M^* = 1.98$, assuming slip on {110} {112} <111> systems. Another frequent Nb orientation is {001} <110>, i.e., the same as the Nb ribbons in the wire drawn composite, thus $M^* = 1.84$ for tensile deformation along the rolling direction.

The copper layers in the Cu-Nb composites appear to develop nearly the same textures as single-phase Cu. A <001> + <111> fibre texture is found in wire drawing [4]. The « brass type » orientation, {110} <112>, is frequent in rolling, where grains with « cube » orientation have also been found, as well as {112} <110> oriented grains at very large strains [31, 42]. The last orientation is absent in single-phase rolled copper. The {112} <111> orientation, by contrast, has not been reported. All published preferred orientations correspond to SADP obtained in TEM observations. No quantitative texture measurements appear to have been made up to now in this family of heavily deformed *in situ* composites. No calculation of M^* orientation factors has been undertaken for the copper textures. « Cube » oriented grains-uniform CRSS, $M = 2.45$ - yield $M^* = 2.0$.

3.2 APPLICATION TO WIRE-DRAWN FINE PEARLITE. — It has been mentioned that the strength of wire drawn fine pearlite shows a Hall-Petch type relationship with the strain-dependent mean transverse spacing. Apparently, this precludes the dominance of the mechanisms leading to equations (17) or (18). On the other hand, according to the precedent

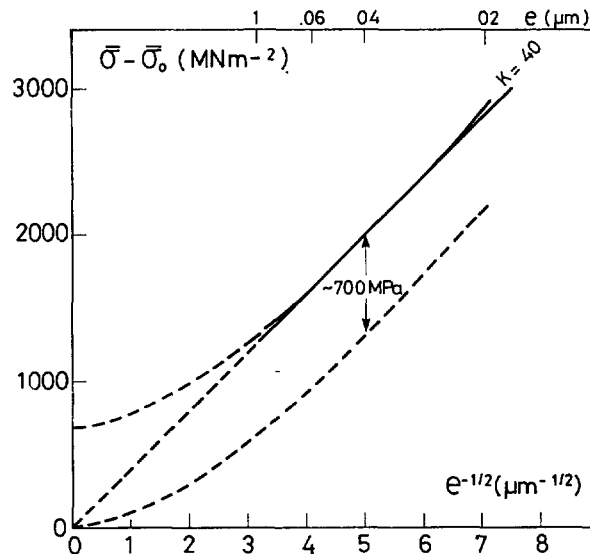


Fig. 7. — Flow stress vs. minimum interlamellar pearlite spacing ($e = S_a/f_a$). Empirical result (Langford, Ref. [22], Hall-Petch slope = 0.40 MNm^{3/2}) and theoretical value, equation (25).

review, the role of statistically stored dislocations in the strengthening of pearlitic ferrite is predicted to be negligible. The empirically derived Hall-Petch behaviour [22] is adequately reproduced by the equation,

$$\bar{\sigma} = \bar{\sigma}_0 + (1 - f_{cem})[M^* \tau_m[(\bar{S}_{min})_\alpha]] + f_{cem}(G_{cem}/10) \tag{25}$$

at least in the range of measured spacings, figure 7 [47]. The logarithmic factor of equation (18) allows for a good mimick of the Hall-Petch relationship along a broad range of spacings. The strength of heavily drawn pearlite is then explained by the additive contributions of the Peierls stress plus solid solution strengthening effects, σ_0 , the ferrite flow stress, controlled by the need of multiplying dislocations in the intralamellar space and a constant contribution from the cementite lamellae, ≈ 700 MPa, which, on account of $f_{cem} \approx 0.12$, corresponds approximately to a cementite strength of the order of $G_{cem}/10$. The latter value is in good agreement with several direct measurements [54-57] of the strength of small cementite crystals.

3.3 APPLICATION TO Cu-20 % vol Nb COMPOSITES. — In the foregoing overview on contributions to the strength of *in situ* composites it was concluded that initially coarse Cu-Nb develops the same structure of statistically stored dislocations as its free-deforming bulk components. Consequently, the CRSS of Cu and Nb in the composite will be determined by the superposition of the strengthening due to a distributed dislocation density and that due to the critical bowing for extruding or multiplying dislocation through the intralamellar corridors, equation (21), and their flow stress will be given by equation (24). Ignoring any other possible strengthening contributions, the flow stress of the composite is calculated to lie between the bounds :

$$0.6[0.8 M_{Cu}^* \tau_b^{Cu}(\bar{S}_{min}^{Cu}) + 0.2 M_{Nb}^* \tau_b^{Nb}(\bar{S}_{min}^{Nb})] \leq (\bar{\sigma} - \bar{\sigma}_{ROM}) \leq 0.6[0.8 M_{Cu}^* \tau_m^{Cu}(\bar{S}_{min}^{Cu}) + 0.2 M_{Nb}^* \tau_m^{Nb}(\bar{S}_{min}^{Nb})] \tag{26}$$

where $\bar{\sigma}_{ROM}$ corresponds to the unmodified ROM.

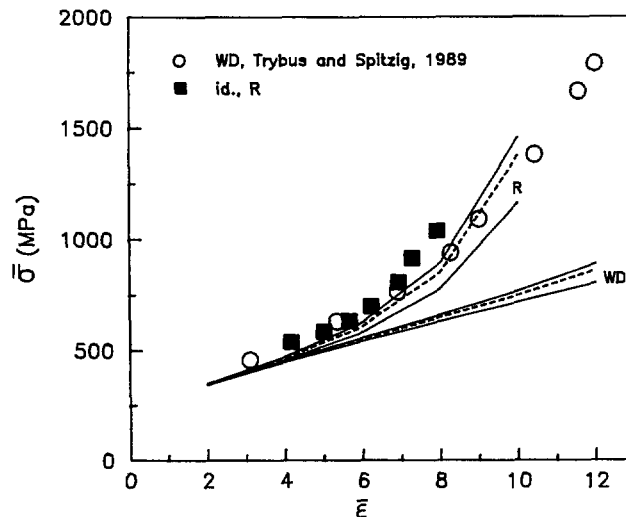


Fig. 8. — Work hardening of Cu-20 % vol. Nb composites in rolling and in wire-drawing. Experimental data from Spitzig *et al.* [3, 4, 31]. Continuous lines : theoretical bounds predicted according to equation (26). Dotted lines : predictions assuming τ_m for Cu and τ_b for Nb.

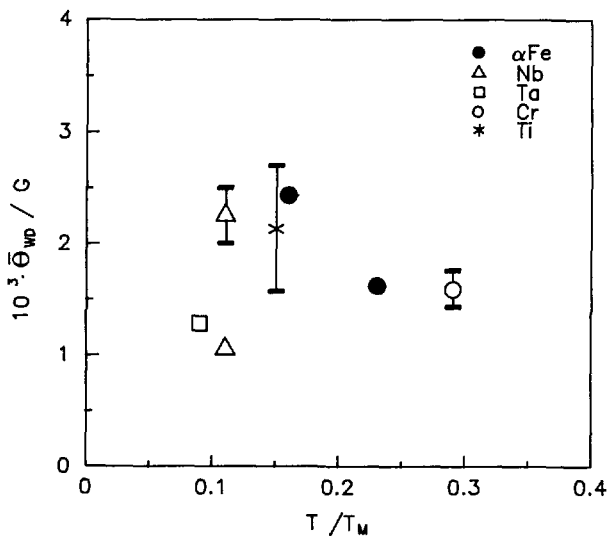


Fig. 9. — Work hardening rate of BCC metals [3, 4, 5, 29, 38] and Ti [60] deformed by wire drawing (i.e., metals showing curling of grains in transverse sections) as a function of homologous temperature.

The lower bound would mean that dislocation multiplication is produced in local regions of high positive internal stresses in both phases. Intermediate situations can be envisaged, e.g., multiplication inside Cu and slip-transfer to Nb through the interface. It seems a reasonable scenario that the easier flow in Cu wraps the thin Nb ribbons with a dislocation net, whose density is instantaneously matched to the level necessary for inducing plastic flow in them. Long range forward stresses will then be acting in Nb and perhaps, ideally, only short range back stresses in the copper matrix (see Refs. 58 and 59 and Saada's paper in this volume).

The flow stress values predicted by equation (26) are compared in figure 8 with the experimental work-hardening curves of Cu-20 % vol. Nb of Spitzig *et al.* [3, 4, 31]. The empirical spacing-strain equations (8) and (9) have been used in the calculation, with $\bar{S}_0^{Cu} = 24.8 \mu\text{m}$ and $\bar{S}_0^{Nb} = 6.2 \mu\text{m}$. A uniform value of $G = 42.5 \text{ GPa}$ has been assumed and — in view of the calculated M^* values, see above — a uniform $M^* = 2$ value has been used for both materials. The work hardening of heavily rolled Cu-20 % vol. Nb is almost completely explained by equation (26), without recourse to any other strengthening contributions. However, on the same premises, the work hardening curve predicted for the wire-drawn composite grossly underestimates the actual experimental behaviour. Similar conclusions were already advanced by Trybus and Spitzig [31]. To reconcile consistently both results, the work hardening measured in excess to the theoretical wire drawing prediction must be ascribed to the curling of the Cu layers imposed by the $\langle 110 \rangle$ Nb ribbons. Otherwise, a totally different explanation must be searched for both deformation modes. The work hardening rate of BCC metals and some Ti alloys during wire drawing — all of them showing the curling of grains in transverse sections — lies from $10^{-3} G$ to $2.5 \times 10^{-3} G$ (Fig. 9). For copper ($T/T_M = 0.22$) a value between $1.5 \times 10^{-3} G$ and $2 \times 10^{-3} G$ should be expected. If such work hardening rate is added to the large-strain stress-strain curve of copper and $\bar{\sigma}_{ROM}$ is thereafter modified for applying equation (26), it is easily seen that the new predicted work hardening curve should be now rather close to the measured one.

4. Conclusions.

— This paper started with a remark about the difficulties for predicting the substructural evolution of single phase materials during plastic straining (a dislocation patterning problem). The same problem remains unsolved for *in situ* composites for both the interphase spacing evolution (a plastic problem to be solved at a mesoscopic level) and the dislocation substructures that can be induced in the two phases. Consequently, a complete work hardening theory is still lacking for both single or two-phase materials.

— The strengthening of ductile two-phase alloys at high strains (*in situ* composites) is rather complex and no single mechanism can be made responsible for it. For a given strain level, flow stress results from superposition of the strengthening effect of the statistically stored dislocation density plus friction, image or internal stresses contributions and from the constraints for dislocation glide and multiplication imposed by interphase barriers. The superposition can be simply integrated in actual models.

— For each phase, below a certain strain threshold dictated by the actual ratio of interphase spacing to interdislocation distance, a transition from a dislocation-dominated state to a barrier controlled one will take place. Thus, the transition depends on the initial interphase spacing, the single-phase bulk work hardening behaviour and the plastic compatibility with the second phase.

— The behaviour of wire-drawn Cu-Nb alloys with starting spacings of the order of, respectively, 30/7 μm is dominated by the density of geometrically necessary dislocations (resolving the continuous curling of Nb and Cu ribbons) up to the maximum attained strains ($\epsilon = 12$). However, in the rolled composite, where « geometrically necessary » dislocations are irrelevant, the direct contribution from interphase barriers is very important. Substantial strength could still be gained in Cu-Nb alloys through initial structure refinement and further straining.

— Fine pearlite ($(S_0)_\alpha \approx 0.07 \mu\text{m}$) at large strains is in the last attainable deformation stage of any *in situ* composite, with one component acting with a whisker-type behaviour (cementite) and the other with its flow stress controlled by the critical stress for activating intraphase dislocation sources.

References

- [1] KOCKS U. F., *J. Eng. Mater. Technol.*, **98** (1976) 76.
- [2] GIL SEVILLANO J., Doctoral dissertation, Katholieke Universiteit Leuven, Leuven (Belgium), 1974.
- [3] SPITZIG W. A. and KROTZ P. D., *Scripta Metall.* **21** (1987) 1143.
- [4] SPITZIG W. A., PELTON A. R. and LAABS F. C., *Acta Metall.* **35** (1987) 2427.
- [5] GIL SEVILLANO J., VAN HOUTTE P. and AERNOUDT E., *Progr. Mater. Sci.* **25** (1980) 69.
- [6] ALBERDI J. M., Doctoral dissertation, Universidad de Navarra, San Sebastian (Spain), 1985.
- [7] HUGHES D. A., Doctoral dissertation, Stanford University (USA), 1986.
- [8] ROLLET A. D., Doctoral dissertation, Los Alamos National Laboratory, Los Alamos, N. M. (USA) 1988.
- [9] HAASEN P., *J. Phys. France* **50** (1989) 2445.
- [10] GIL SEVILLANO J., Proc. II World Basque Congress, Conference on New Structural Materials, P. 137. Gob. Vasco, Serv. Central de Public., Vitoria (Spain) 1988.
- [11] THOMPSON, S. J. and FLEWITT, P. E. J., *J. Less Common Met.*, **40** (1975) 269.
- [12] FROST H. J. and ASHBY M. F., « Deformation Mechanisms Maps » (Pergamon Press, Oxford, U.K., 1982.

- [13] HARBISON J. P. and BEVK J., *J. Appl. Phys.* **48** (1977) 5180.
- [14] BEVK J., HARBISON J. P. and BELL J. L., *J. Appl. Phys.* **49** (1978) 12.
- [15] KUHLMANN-WILSDORF D. and HARRIGAN Jr. W. C., Eds., « New Developments and Applications in Composites ». TMS-AIME, Warrendale, PA (USA) 1979.
- [16] WASSERMANN G., Proc. 2nd Int. Conf. On the Strength of Metals and Alloys (ICSMA 2), vol. III, p. 1988. ASM, Metals Park, Ohio (USA) 1970.
- [17] FROMMEYER G. and WASSERMANN G., *Acta Metall.* **23** (1975) 1353.
- [18] CLINE H. E., STRAUSS B. P., ROSE R. M. and WULFF J., *Trans. ASM* **59** (1966) 132.
- [19] RIVEROS HUCKSTADT R., Master dissertation, ESII, University of Navarra, San Sebastian (Spain) 1986.
- [20] EMBURY J. D. and FISHER R. M., *Acta Metall.* **14** (1966) 147.
- [21] LANGFORD G., *Metall. Trans.* **1** (1970) 465.
- [22] LANGFORD G., *Metall. Trans. A* **8A** (1977) 861.
- [23] VERHOEVEN J. D., SCHMIDT F. A., GIBSON E. D. and SPITZIG W. A., *J. Metals* **38** (1986) 20.
- [24] ROLLET A. D., KOCKS V. F., EMBURY J. D., STOUT M. G. and DOHERTY R. D., « Strength of Metals and Alloys », ICSMA8 Proc., vol. 1, p. 433. P. O. Dettumen, T. K. Lepistö and M. E. Lehtonen, Eds. (Pergamon Press, Oxford UK) 1988.
- [25] FUNKENBUSCH P. D. and COURTNEY T. H., *Scripta Metall.* **23** (1989) 1719.
- [26] NABARRO F. R. N., BASINSKI A. S. and HOLT D. B., *Advances in Physics* **13** (1964) 193.
- [27] ASHBY M. F., « Strengthening Methods in Crystals », p. 137. A. Kelly and R. B. Nicholson, Eds., Applied Science, London (UK) 1970.
- [28] KOCKS U. F., « Dislocations and Properties of Real Materials », p. 125. The Institute of Metals, London (UK) 1985.
- [29] LANGFORD G., Doctoral dissertation, Massachusetts Institute of Technology (USA), 1966.
- [30] MATSCHASS F., *Wiss. Z. Tech. Univ. Magdeburg* **32** (1988) 21.
- [31] TRYBUS C. L. and SPITZIG W. A., *Acta Metall.* **37** (1989) 1971.
- [32] SUE J. J., VERHOEVEN J. D., GIBSON E. D., OSTENSON J. E. and FINNEMORE D. K., *Acta Metall.* **29** (1981) 1971.
- [33] SPITZIG W. A. and KROTZ P. D., *Acta Metall.* **36** (1988) 1709.
- [34] FUNKENBUSCH P. D., COURTNEY T. H. and KUBISCH D. G., *Scripta Metall.* **18** (1984) 1099.
- [35] BORDEAUX F. and YAVARI JR., *Z. Metallkunde* **81** (1990) 130.
- [36] EMBURY J. D., KEH A. S. and FISHER R. M., *Trans. AIME* **236** (1966) 1252.
- [37] HU H., « Textures in Research and Practice », p. 200. J. Grewen and G. Wassermann, Eds. (Springer Verlag, Berlin, FRG) 1969.
- [38] LANGFORD G. and COHEN M., *Trans. ASM* **62** (1969) 623.
- [39] RACK H. J. and COHEN M., *Mater. Sci. Eng.* **6** (1970) 320.
- [40] KARASEK K. R. and BEVK J., *Scripta Metall.* **14** (1980) 431.
- [41] FROMMEYER G. and BRION H. G., *Phys. Stat. Sol. (a)* **66** (1981) 559.
- [42] SPITZIG W. A., *Scripta Metall.* **23** (1989) 1177.
- [43] FUNKENBUSCH P. D. and COURTNEY T. H., *Acta Metall.* **33** (1985) 913.
- [44] FUNKENBUSCH P. D., LEE J. K. and COURTNEY T. H., *Metall. Trans. A* **18A** (1987) 1249.
- [45] LI J. C. M. and CHOU Y. T., *Metall. Trans.* **1** (1970) 1145.
- [46] EVERETT R. K., *Scripta Metall.* **22** (1988) 1227.
- [47] GIL SEVILLANO J., Proc. 5th Int. Conf. on The Strength of Metals and Alloys (ICSMA 5) vol. 2, p. 819, P. Haasen, V. Gerold and G. Kosterz, Eds. (Pergamon Press, Oxford, UK) 1978.
- [48] ECKELMEYER K. E. and HERTZBERG R. W., *Metall. Trans.* **3** (1972) 609.
- [49] KOEHLER J. S., *Phys. Review B* **2** (1970) 547.
- [50] KAMAT S. V. and HIRTH J. P., *Scripta Metall.* **21** (1987) 1587.
- [51] GIL SEVILLANO J., VAN HOUTTE P. and AERNOUDT E., Proc. 5th Int. Conf. on Textures of Materials (ICOTOM 5), vol. II, p. 495. G. Gottstein and K. Lücke, Eds. (Springer Verlag, Berlin, FRG) 1978.
- [52] VAN HOUTTE P., *Text. Microstr.*, **8-9** (1988) 313.
- [53] VANDERMEER R. A. and OGLE J. C., *Trans. AIME* **242** (1968) 1317.
- [54] WEBB W. W. and FORGENG W. D., *Acta Metall.* **6** (1958) 462.

- [55] COLLINS M. J. and WOODFORD D. A., *J. Iron Steel Inst.* **203** (1983) 184.
- [56] KAGAWA A. and OKAMOTO T., *J. Mater. Sci.* **18** (1983) 225.
- [57] INOUE A., OGURA T. and MASUMOTO T., *Trans. J.I.M.* **17** (1976) 664.
- [58] TORREALDEA F. J. and GIL SEVILLANO J., Proc. 6th Int. Conf. on The Strength of Metals and Alloys, vol. I, p. 547, R. C. Gifkins, Ed. (Pergamon Press, Oxford, UK), 1983.
- [59] MARTÍN MEIZOSO A., GIL SEVILLANO J., FUENTES PÉREZ M., *Rev. Metalurgia* **20** (1984) 205.
- [60] BISWAS C., COHEN M. and BREEDIS J. F., Proc. 3rd Int. Conf. on Strength of Metals and Alloys (ICSMA3), vol. I, p. 16, Cambridge (UK) 1973.